RAPID COMMUNICATIONS

PHYSICAL REVIEW B VOLUME 30, NUMBER 3 1 AUGUST 1984

Zero-field muon-spin relaxation in *Cu*Mn spin-glasses compared with neutron and susceptibility experiments

Y. J. Uemura
Brookhaven National Laboratory, Upton, New York 11973

D. R. Harshman, M. Senba, and E. J. Ansaldo*
TRIUMF, University of British Columbia, Vancouver, British Columbia, Canada

A. P. Murani
Institute Laue Langevin, 156 X, F-38042 Grenoble, France

(Received 24 April 1984)

Zero-field muon-spin relaxation has been measured in *Cu*Mn spin-glasses (5 at.% and 3 at.%) using the surface muon beam. Dynamic correlation time and static spin polarization of Mn moments, determined at $0.1T_g \sim 3T_g$, are consistent with neutron-spin-echo and ac-susceptibility measurements on the same specimens reported in different time windows. The combination of these three experiments demonstrates the spin freezing of *Cu*Mn with the time-persistent Mn polarization below T_g.

For the study of the spin dynamics of spin-glasses,[1] positive muon-spin relaxation (μ^+SR) has recently been shown to be a powerful new probe[2-5] among other standard experimental methods. Its capability of zero-field measurements[6] is especially suited to spin-glasses where the sharp cusp of ac susceptibility χ_{ac} at the cusp temperature T_g is rounded by the application of small external magnetic fields. In the zero-field μSR (ZF-μSR) experiments applied to spin-glasses *Cu*Mn and *Au*Fe (~ 1 at.%, Ref. 6) and to *Ag*Mn,[4] the spin fluctuation of the Mn (or Fe) moment was found to slow down rapidly when T_g was approached from higher temperatures, and to become almost static below T_g within the simplest approximation of Markovian fluctuations. Since a subsequent μSR measurement with longitudinal external magnetic fields[3] revealed that the static and dynamic random fields from Mn moments coexist at each muon site below T_g, attempts were made[4,7] to deduce the amplitude $a_s = \gamma_\mu H_s$ ($\gamma_\mu = 8.5\times 10^4$/sec Oe) of the static random fields H_s in ZF-μSR. The statistical accuracy of a_s and the detailed data analyses were, however, limited by the dead time $t \sim 30$ nsec of the μSR spectrometers used in the previous studies, and this dead time also made it difficult to apply ZF-μSR to dilute-alloy spin-glasses with impurity concentration c higher than 2 at.%.

Avoiding these difficulties by using the "surface muon" beam of TRIUMF, we have performed ZF-μSR measurements in 5% and 3% *Cu*Mn ($T_g = 27.4$ and 20.0 K; prepared by quenching from $T = 830\,^\circ$C), and describe the results in this article. We used the specimens cut from the same *Cu*Mn samples examined by neutron-spin-echo (NSE) (5%),[8] neutron time-of-flight (3%),[9] and ac-susceptibility (χ_{ac}) (Ref. 8) measurements, so that the findings of neutrons, μSR, and χ_{ac} can be directly compared and combined. Thanks to the low incident energy 4.1 MeV, surface muons are fully separated from the associated beam particles with a Wien dc separator, and are completely stopped in the specimen within the range ~ 200 mg/cm^2.[10] These features allow us to remove the positron counters from the anticoincidence of the "stopped muon" logics, and to observe the time spectrum of muon-decay positrons free from the dead time near $t = 0$ with very low background. Positron intensities were recorded by two sets of counters placed in the forward (F) and backward (B) directions of the specimen, and the muon-spin relaxation function $G_z(t)$ was measured via the asymmetry F(t)/B(t) in the entire time region of 10 nsec $< t < 10\ \mu$sec with very high statistics, as shown in Fig. 1 for 5% *Cu*Mn. The temperature was stabilized to within ± 0.1 K at each point.

When we assume the Mn moment S to follow a simple time-correlation function with Edwards-Anderson order parameter Q[11]

$$\langle S(t)S(0)\rangle / \langle S(0)^2\rangle = (1-Q)\exp(-\nu t) + Q \ , \quad (1)$$

the expected theoretical form of $G_z(t)$ can be calculated analytically as described in Refs. 6 and 7 to yield

$$G_z(t) = \tfrac{1}{3}\exp(-\sqrt{\lambda_d t}\,) + \tfrac{2}{3}\left(1 - \frac{a_s^2 t^2}{(\lambda_d t + a_s^2 t^2)^{1/2}}\right) \times \exp[-(\lambda_d t + a_s^2 t^2)^{1/2}] \ , \quad (2)$$

$$\lambda_d = 4a_d^2/\nu, \quad a_s^2/(a_s^2 + a_d^2) = Q \ ,$$

where a_s and a_d, respectively, represent the averaged amplitude of static and dynamic random local fields at the muon site. For the purely dynamic case where $a_s \to 0$ and $Q \to 0$, this function exhibits a "root-exponential" decay $G_z(t) = \exp(-\sqrt{\lambda_d t}\,)$ similar to $G_z^{SG}(t)$ of Ref. 6. The static effect is reflected in the quick initial decay of $G_z(t)$ followed by the $\frac{1}{3}$ "tail," as indicated by the characteristic static line shape

$$G_z(t) = \tfrac{1}{3} + \tfrac{2}{3}(1 - a_s t)\exp(-a_s t)$$

obtained for $a_d \to 0$, $Q \to 1$. These features of line shapes are superimposed when static and dynamic random fields are coexisting. To include the effect of nuclear dipolar fields, Eq. (2) has to be multiplied with Kubo-Toyabe func-

 ©1984 The American Physical Society

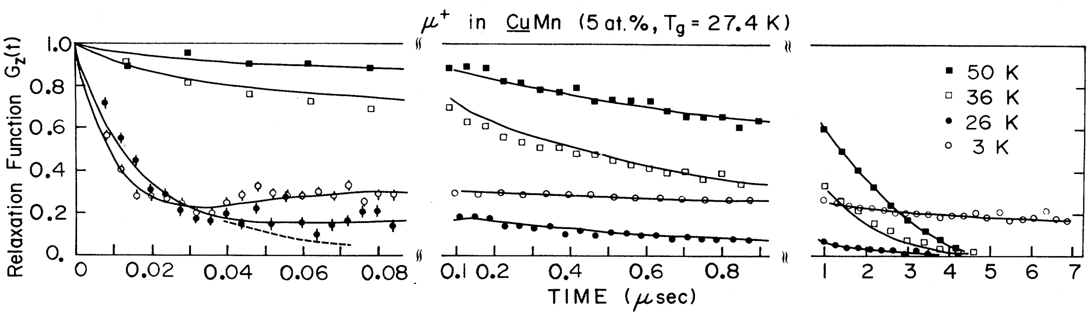

FIG. 1. Muon-spin relaxation function $G_z(t)$ observed in a spin-glass *Cu*Mn (5 at.%, $T_g=27.4$ K) in zero field. The error bars of the data are within the size of each point unless indicated. The solid lines show the best-fit curves with Eq. (2) [for $T=36$ and 50 K, Eq. (2) was multiplied with Kubo-Toyabe function for pure Cu]. The broken line at $T=26$ K illustrates the decay of $G_z(t)$ expected when we assume no persisting field ($a_s \rightarrow 0$).

tion for a pure Cu system[6] when $a_s \lesssim 0.5\ \mu\text{sec}^{-1}$.

Varying a_s and λ_d as the only free parameters, the observed data of $G_z(t)$ were fitted to this function. The best-fit curve, shown by the solid lines of Fig. 1, agrees well with the experiment, and this justifies the use of Eq. (2) in the analysis. Small differences, noticed at $T=26$ and 36 K of Fig. 1, might be suggesting the spin dynamics to be more complicated than Eq. (1) around T_g. The extracted best-fit values of a_s and λ_d are shown in Fig. 2, together with some results of 1% *Cu*Mn. Although we made no *a priori* assumptions, a_s exhibits nonzero values only below T_g of each specimen, and increases with decreasing temperature towards the full amplitude $a_0=(a_s^2+a_d^2)^{1/2}=a_s(T=0)$ of random fields. Assuming the full polarization of Mn moments with $2\sqrt{S(S+1)}=5.0$ at $T=0$ in Eqs. (12) and (13) of Ref. 6, the theoretical value of a_0 can be calculated from the lattice sum to be $a_0=c\times 14\ \mu\text{sec}^{-1}$, which agrees well with the observed quantity $a_0(5\%)=70\ \mu\text{sec}^{-1}$ and $a_0(3\%)=50\ \mu\text{sec}^{-1}$. Since a_s/a_0 corresponds to $\sqrt{Q}$, Fig. 2(a) represents the static polarization $P=\sqrt{Q}$ of Mn moments measured by μSR. To cause the quick initial damping of $G_z(t)$, such a polarization has to be "static" only up to the time $t=1/a_s=20$–100 nsec. The observed "tail" of $G_z(t)$, however, indicates the field of a_s to be persisting up to $t=1$–$5\ \mu$sec. Without the persisting field, indeed, $G_z(t)$ should have decayed as illustrated by the broken line of Fig. 1 at $T=26$ K.

The dynamic depolarization rate λ_d in Fig. 2(b) increases rapidly when T_g is approached both from higher and lower temperatures. Above T_g where $a_s=0$ and $a_d=a_0$, the correlation time $\tau_c=1/\nu$ of Mn moments can be deduced from λ_d as $\tau_c=\lambda_d/4a_0^2$. When we compare τ_c with the power law $\tau_c=\tau_0[T/(T-T_g)]^z$ above T_g, we obtained $\tau_0=8\times10^{-13}$ sec, $z=2.9$ for 5% *Cu*Mn, and $\tau_0=7\times10^{-13}$ sec, $z=2.6$ for 3%*Cu*Mn from the corresponding fit to λ_d shown by the solid lines in Fig. 2(b). Since it becomes increasingly difficult to obtain reliable values of a_d at lower temperatures, we will just give a rough estimate $\nu\sim10^{10}$/sec for the decay rate ν of the dynamic random fields below T_g. These results of a_s and λ_d are consistent with earlier works in *Au*Fe (Refs. 6 and 7) and *Ag*Mn,[4] while the accuracy has been improved thanks to the full observation of $G_z(t)$.

In Fig. 3, we compared the findings of ZF-μSR of 5% *Cu*Mn to the time-correlation function $\xi(t)$ of Mn moments measured by neutron-spin-echo and ac-susceptibility[8] for the same specimen. Since $\xi(t)$ cannot directly be measured by μSR, we plotted our results of τ_c above T_g at $\xi(t=\tau_c)=1/e$ as the representative points. A few points

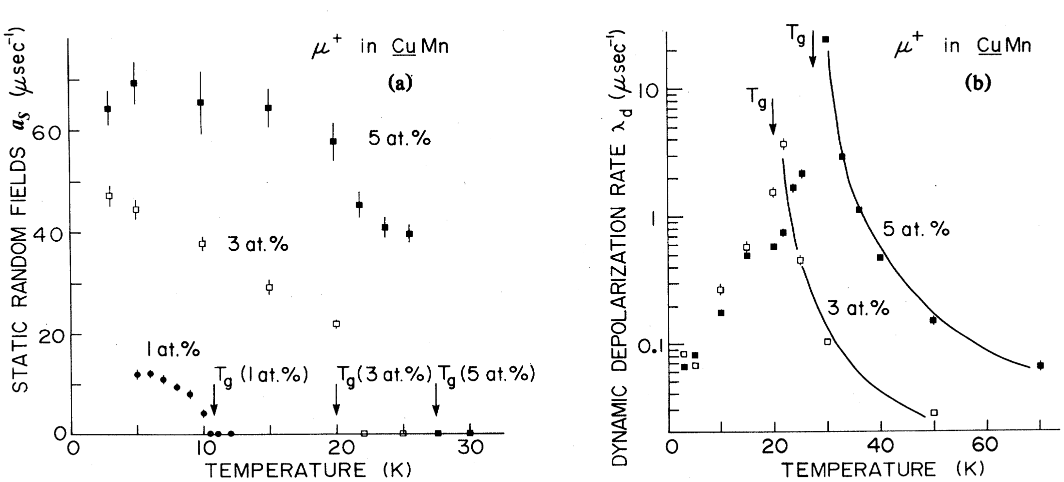

FIG. 2. (a) Averaged amplitude a_s of static random local field at the muon site, and (b) the dynamic muon-spin depolarization rate λ_d, deduced from zero-field μSR experiments in *Cu*Mn spin-glasses by fitting the data with Eq. (2). The solid line of (b) corresponds to $\lambda_d \propto [T/(T-T_g)]^z$ with $z=2.9$ for 5% and $z=2.6$ for 3% *Cu*Mn.

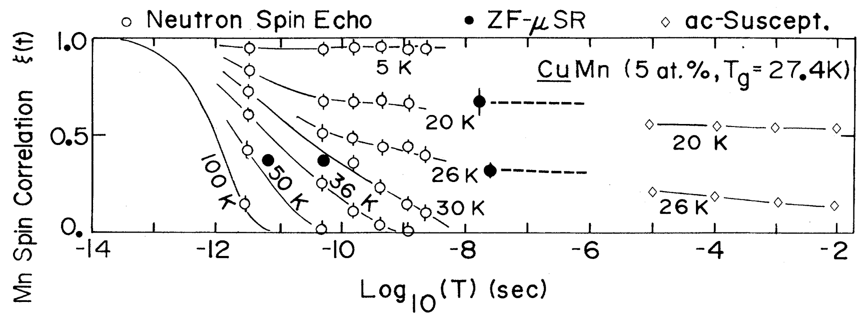

FIG. 3. Time-correlation function $\xi(t)$ of Mn spin fluctuation in a spin-glass *Cu*Mn (5%, $T_g = 27.4$ K) measured by neutron-spin-echo (Ref. 8) and ac susceptibility (Ref. 8), where the results of ZF-μSR are compared. At $T=50$ and 36 K, μSR data are plotted at $\xi(t=\tau_c)=1/e$ representing the measured correlation time τ_c, while the static polarization are plotted at $\xi(1/a_s)=(a_s/a_0)^2$ at $T=26$ and 20 K together with the broken line indicating the persistency of a_s expected from the "tail" of $G_z(t)$.

are also plotted at $\xi(t=1/a_s)=(a_s/a_0)^2$ by using the static amplitude a_s below T_g, where the attached broken lines indicate the persistency of the static component expected from the "tail" of $G_z(t)$. Three independent zero-field results of NSE, ZF-μSR, and χ_{ac} agree very well, and the combined time correlation demonstrates Mn moments to slow down rapidly above T_g and to possess a long-time persisting component below T_g.

The comparison in Fig. 3 also helps us to roughly distinguish between the two different pictures of spin freezings below T_g, i.e., (a) "homogeneous freezing" where all the Mn moments have equivalent static polarization $P=\sqrt{Q}$, and (b) "extremely inhomogeneous freezing" where, for example, 10 spins out of 100 are completely frozen ($Q=1$) while the remaining 90 spins are paramagnetic ($Q=0$). In the homogeneous picture (a), the static field a_s of μSR is linearly while the elastic intensity I_{el} of NSE and χ_{ac} are quadratically proportional to P. In contrast, a_s, I_{el}, and χ_{ac} are all linearly proportional to the number of frozen spins in the inhomogeneous case of (b).[7] Therefore, the good agreement of the squared quantity $(a_s/a_0)^2$ to I_{el} and χ_{ac}, shown in Fig. 3 below T_g, tends to support the homogeneous freezing.

A deviation of $\xi(t)$ from Eq. (1) is seen in the NSE data, and is studied also in some other experiments.[9,12] We have, however, confined ourselves within the approximation of Eqs. (1) and (2) in the analysis in order to grasp general features using a reliable standard approach.[13] In conclusion, the present experiment has provided direct information on the dynamics of Mn moments in the time region inaccessible for NSE and χ_{ac}, and the combination of the three experiments have enlightened a rather homogeneous spin freezing of *Cu*Mn with a persistent static Mn polarization below T_g.

We would like to thank F. Mezei, J. L. Tholence, J. H. Brewer, K. M. Crowe, E. W. Vogt, and T. Yamazaki for stimulating discussions and encouragement. Work done at Brookhaven was supported by the Division of Materials Science, U.S. Department of Energy under Contract No. DE-AC02-76CH00016.

---

*On leave from Department of Physics, University of Saskatchewan, Saskatchewan, Canada 57N 0W0.

[1]J. A. Mydosh, J. Magn. Magn. Mater. **7**, 237 (1978); V. Cannella and J. A. Mydosh, Phys. Rev. B **6**, 4220 (1972).

[2]D. E. Murnick, A. T. Fiory, and W. J. Kossler, Phys. Rev. Lett. **36**, 100 (1976).

[3]Y. J. Uemura and T. Yamazaki, Physica **109&110B**, 1915 (1982).

[4]R. H. Heffner, M. Leon, M. Schillaci, D. E. MacLaughlin, and S. A. Dodds, J. Appl. Phys. **53**, 2174 (1982).

[5]K. Emmerich and Ch. Schwink, Hyper. Inter. **8**, 767 (1981); K. Emmerich, F. N. Gygax, A. Hintermann, H. Pinkvos, A. Schenck, Ch. Schwink, and W. Studer, J. Magn. Magn. Mater. **31–34**, 1361 (1983).

[6]Y. J. Uemura, Hyper. Inter. **8**, 739 (1981); Y. J. Uemura, T. Yamazaki, R. S. Hayano, R. Nakai, and C. Y. Huang, Phys. Rev. Lett. **45**, 583 (1980).

[7]Y. J. Uemura, Ph.D. thesis, University of Tokyo, 1982; Y. J. Uemura and T. Yamazaki, J. Magn. Magn. Mater. **31–34**, 1359 (1983); Y. J. Uemura, Hyper Inter. **17–19**, 447 (1984).

[8]F. Mezei and A. P. Murani, J. Magn. Magn. Mater. **14**, 211 (1979); A. P. Murani, F. Mezei, and J. L. Tholence, Physica B **108**, 1384 (1981).

[9]A. P. Murani, J. Magn. Magn. Mater. **22**, 271 (1981).

[10]J. H. Brewer, Hyper. Inter. **8**, 831 (1981).

[11]S. F. Edwards and P. W. Anderson, J. Phys. F **5**, 965 (1975); **6**, 1927 (1976).

[12]D. E. MacLaughlin, L. C. Gupta, D. W. Cooke, R. H. Heffner, M. Leon, and M. E. Schillaci, Phys. Rev. Lett. **51**, 927 (1983); R. H. Heffner, M. Leon, and D. E. MacLaughlin, Hyper. Inter. **17–19**, 457 (1984).

[13]References 3, 4, 6, 7, and 12 employ similar approaches in data analyses, by assuming "root-exponential" relaxation functions based on Eq. (1).